Sol-gel derived ionic copper-doped microstructured optical fiber: a potential selective ultraviolet radiation dosimeter

Hicham El Hamzaoui, Youcef Ouerdane, Laurent Bigot, Géraud Bouwmans, Bruno Capoen, Aziz Boukenter, Sylvain Girard, Mohamed Bouazaoui

Sol-gel derived ionic copper-doped microstructured optical fiber: a potential selective ultraviolet radiation dosimeter

Hicham El Hamzaoui,[1] Youcef Ouerdane,[2] Laurent Bigot,[1] Géraud Bouwmans,[1] Bruno Capoen,[1] Aziz Boukenter,[2] Sylvain Girard[2] and Mohamed Bouazaoui[1,*]

[1]*Laboratoire PhLAM/IRCICA, CNRS-Université Lille 1, F-59655 Villeneuve d'Ascq Cedex, France*
[2]*Laboratoire Hubert Curien, CNRS-Université Jean Monnet, F-42000 Saint-Etienne, France*
[*]*mohamed.bouazaoui@phlam.univ-lille1.fr*

Abstract: We report the fabrication and characterization of a photonic crystal fiber (PCF) having a sol-gel core doped with ionic copper. Optical measurements demonstrate that the ionic copper is preserved in the silica glass all along the preparation steps up to fiber drawing. The photoluminescence results clearly show that such an ionic copper-doped fiber constitutes a potential candidate for UV-C (200-280 nm) radiation dosimetry. Indeed, the Cu^{+}-related visible photoluminescence of the fiber shows a linear response to 244 nm light excitation measured for an irradiation power up to 2.7 mW at least on the Cu-doped PCF core. Moreover, this response was found to be fully reversible within the measurement accuracy of this study (± 1%), underlying the remarkable stability of copper in the Cu^{+} oxidation state within the pure silica core prepared by a sol-gel route. This reversibility offers possibilities for the achievement of reusable real-time optical fiber UV-C dosimeters.

OCIS codes: (160.6060) Solgel; (160.6990) Transition-metal-doped materials; (060.2280) Fiber design and fabrication; (060.5295) Photonic crystal fibers; (060.2370) Fiber optics sensors; (260.7190) Ultraviolet.

References and links

1. S. Gómez, I. Urra, R. Valiente, and F. Rodríguez, "Spectroscopic study of Cu^{2+}/Cu^{+} doubly doped and highly transmitting glasses for solar spectral transformation," Sol. Energy Mater. Sol. Cells **95**(8), 2018–2022 (2011).
2. O. B. Miled, C. Sanchez, and J. Livage, "Spectroscopic studies and evanescent optical fibre wave sensing of Cu^{2+} based on activated mesostructured silica matrix," J. Mater. Sci. **40**(17), 4523–4530 (2005).
3. N. S. Dhoble, S. P. Pupalwar, S. J. Dhoble, A. K. Upadhyay, and R. S. Kher, "Lyoluminescence and mechanoluminescence of Cu^{+} activated $LiKSO_4$ phosphors for radiation dosimetry," Radiat. Meas. **46**(12), 1890–1893 (2011).
4. B. L. Justus, P. Falkenstein, A. L. Huston, M. C. Plazas, H. Ning, and R. W. Miller, "Gated fiber-optic-coupled detector for *in vivo* real-time radiation dosimetry," Appl. Opt. **43**(8), 1663–1668 (2004).
5. S. Gomez, I. Urra, R. Valiente, and F. Rodriguez, "Spectroscopic study of Cu^{2+} and Cu^{+} ions in high-transmission glass. Electronic structure and Cu^{2+}/Cu^{+} concentrations," J. Phys. Condens. Matter **22**(29), 295505 (2010).
6. S. A. Payne, L. L. Chase, L. K. Smith, W. L. Kway, and W. F. Krupke, "Infrared Cross-Section Measurements for Crystals Doped with Er^{3+}, Tm^{3+}, and Ho^{3+}," IEEE J. Quantum Electron. **28**(11), 2619–2630 (1992).
7. A. Michnik, K. Michalik, and Z. Drzazga, "Effect of UVC radiation on conformational restructuring of human serum albumin," J. Photochem. Photobiol. B **90**(3), 170–178 (2008).
8. H. P. Leenhouts and K. H. Chadwick, *Human Exposure to Ultraviolet Radiation: Risks and Regulations*, Eds: W F Passchier and B F Bosnjakovic (Elsevier, 1987).
9. C. E. Andersen, J. M. Edmund, and S. M. S. Damkjær, "Precision of RL/OSL medical dosimetry with fiber-coupled Al_2O_3:C: Influence of readout delay and temperature variations," Radiat. Meas. **45**(3-6), 653–657 (2010).
10. G. V. M. Williams and S. G. Raymond, "Fiber-optic-coupled $RbMgF_3:Eu^{2+}$ for remote radiation dosimetry," Radiat. Meas. **46**(10), 1099–1102 (2011).
11. A. Bjarklev, J. Broeng, and A. S. Bjarklev, *Photonic Crystal Fibres* (Kluwer Academic, 2003).
12. H. El Hamzaoui, L. Courtheoux, V. Nguyen, E. Berrier, A. Favre, L. Bigot, M. Bouazaoui, and B. Capoen, "From porous silica xerogels to bulk optical glasses: The control of densification," Mater. Chem. Phys. **121**(1-2), 83–88 (2010).

#176707 - $15.00 USD Received 21 Sep 2012; revised 21 Nov 2012; accepted 21 Nov 2012; published 20 Dec 2012

13. H. El Hamzaoui, L. Bigot, G. Bouwmans, I. Razdobreev, M. Bouazaoui, and B. Capoen, "From molecular precursors in solution to microstructured optical fiber: a Sol-gel polymeric route," Opt. Mater. Express **1**(2), 234–242 (2011).
14. P. S. J. Russell, "Photonic-Crystal Fibers," J. Lightwave Technol. **24**(12), 4729–4749 (2006).
15. Y. Fujimoto and M. Nakatsuka, "Spectroscopic properties and quantum yield of Cu-doped SiO_2 glass," J. Lumin. **75**(3), 213–219 (1997).
16. Q. Zhang, G. Chen, G. Dong, G. Zhang, X. Liu, J. Qiu, Q. Zhou, Q. Chen, and D. Chen, "The reduction of Cu^{2+} to Cu^{+} and optical properties of Cu^{+} ions in Cu-doped and Cu/Al-codoped high silica glasses sintered in an air atmosphere," Chem. Phys. Lett. **482**(4-6), 228–233 (2009).
17. E. Borsella, A. Dal Vecchio, M. A. Garcia, C. Sada, F. Gonella, R. Polloni, A. Quaranta, and L. J. G. W. van Wilderen, "Copper doping of silicate glasses by the ion-exchange technique: A photoluminescence spectroscopy study," J. Appl. Phys. **91**(1), 90–98 (2002).
18. A. Lin, B. H. Kim, D. S. Moon, Y. Chung, and W.-T. Han, "Cu^{2+}-doped germano-silicate glass fiber with high resonant nonlinearity," Opt. Express **15**(7), 3665–3672 (2007).
19. J. Kaufmann and C. Rüssel, "Thermodynamics of the Cu^{+}/Cu^{2+}-redox equilibrium in alumosilicate melts," J. Non-Cryst. Solids **356**(33-34), 1615–1619 (2010).
20. Y. Sakurai, "The 3.1 eV photoluminescence band in oxygen-deficient silica glass," J. Non-Cryst. Solids **271**(3), 218–223 (2000).
21. S. Munekuni, T. Yamanaka, Y. Shimogaichi, R. Tohmon, Y. Ohki, K. Nagasawa, and Y. Hama, "Various types of non bridging oxygen hole center in high-purity silica glass," J. Appl. Phys. **68**, 1212–1217 (1990).
22. Y. Sakurai, K. Nagasawa, H. Nishikawa, and Y. Ohki, "Characteristic red photoluminescence band in oxygen-deficient silica glass," J. Appl. Phys. **86**(1), 370–373 (1999).
23. Y. Hibino and H. Hanafusa, "Defect structure and formation mechanism of drawing-induced absorption at 630 nm in silica optical fibers," J. Appl. Phys. **60**(5), 1797–1801 (1986).
24. E. J. Friebele, G. H. Sigel, Jr., and D. L. Griscom, "Drawinginduced defect centers in a fused silica core fiber," Appl. Phys. Lett. **28**(9), 516–518 (1976).
25. G. H. Sigel, Jr. and M. G. Marrone, "Photoluminescence in as-drawn and irradiated silica optical fibers: an assessment of the role of non-bridging oxygen defect centers," J. Non-Cryst. Solids **45**(2), 235–247 (1981).
26. P. Kaiser, "Drawing-induced coloration in vitreous silica fibers," J. Opt. Soc. Am. **64**(4), 475–481 (1974).
27. J.-W. Lee, G. H. Sigel, Jr., and J. Li, "Processing-induced defects in optical waveguide materials," J. Non-Cryst. Solids **239**(1-3), 57–65 (1998).
28. M. A. García, E. Borsella, S. E. Paje, J. Llopis, M. A. Villegas, and R. Polloni, "Luminescence time decay from Cu^{+} ions in Sol-gel silica coatings," J. Lumin. **93**(3), 253–259 (2001).
29. M. Neff, V. Romano, and W. Lüthy, "Metal-doped fibres for broadband emission: Fabrication with granulated oxides," Opt. Mater. **31**(2), 247–251 (2008).

1. Introduction

Recently, extensive efforts have been devoted to transition metal ion-doped photonic materials owing to their potential optical applications. Thereby, ionic copper-based nanocomposites present a promising route to improve the efficiency of light collection in solar cells [1], and in chemical sensing using evanescent waves in optical fibers [2]. Moreover, if ionic copper-activated materials have been used in ionizing radiation dosimetry [3,4], they could be also used for non-ionizing radiation sensing via the Optically Stimulated Luminescence (OSL) effect. In fact, it is known that the presence of Cu^{+} ions in different matrices induces useful optical properties. They present large absorption cross section in the UV region (~2.5 x 10^{-17} cm^2) [5], which is at least two order of magnitude higher than those of trivalent rare-earth ions (<10^{-19} cm^2) for example [6]. Moreover, The Cu^{+} ions absorb selectively the UV-C radiation, which is of great interest due to their associated biological hazards [7,8].

Optical fiber-based dosimeters present a key advantage over their electronic counterparts because they operate without electrical or radio-frequency interference. Moreover the fiber architecture is suitable for environmental monitoring, or applications requiring monitoring over a long distance. Two kinds of conventional optical fiber-based dosimeters have been so far developed. In the first one, the radiation-sensitive element is a length of specially formulated quartz fiber. This one is attached to a length of another optical fiber that is used to guide the optical signal to the detector [4]. The second one consists of small bulk radiation-sensitive material coupled with an optical fiber. In this latter case, the fiber acts only as a waveguide to carry an optical signal from the sensing material to a detector [9,10].

Due to the multiple degrees of freedom in designing and controlling their optical properties, PCFs can be considered as an alternative solution to the conventional optical fiber technology in many applications [11]. Besides, sol-gel synthesis has become a mature and

#176707 - $15.00 USD Received 21 Sep 2012; revised 21 Nov 2012; accepted 21 Nov 2012; published 20 Dec 2012

pertinent technology in the preparation of optical materials such as silica-based glasses and nanocomposites. This method presents various advantages over the traditional techniques, such as a greater homogeneity, a higher purity, lower processing temperatures and a better control of the glass properties. In this manner, we have recently prepared high purity-grade silica glass rods using the polymeric sol-gel route. These sol-gel silica rods with a large cross section have been used as starting materials to achieve passive or active PCFs for efficient Er-doped fiber amplifiers [12,13].

To the best of our knowledge, this paper is the first report of a pure silica solid core PCF, doped with ionic copper and prepared using a polymeric sol-gel route. This fiber exhibits interesting reversible optical properties that could be exploited in UV-C radiation dosimetry. The all-fibered sensor concept has a simple configuration in which the same fiber simultaneously acts as the waveguide and as the sensitive material.

2. Experimental

The first step of the fabrication consists in the synthesis of a cylindrical rod by the sol-gel route. This technique was chosen because it enables to achieve transparent glasses at low temperatures, that is to say several hundred of degrees below the reaction temperature required in the conventional industrial Chemical Vapor Deposition process. Then, the obtained rod was integrated in an air/silica PCF structure using the conventional stack-and-draw process [14].

Porous silica monoliths, shaped as cylinders, were prepared from tetraethylorthosilicate (TEOS), as already described elsewhere [12,13]. One of those porous monoliths, exhibiting interconnected nanometric pores, was doped by soaking it into a copper salt solution. Then, the sample was taken out and dried for several hours to remove solvents. The resulting doped xerogel was then densified under air atmosphere at 1200°C. In this way, a pale green-colored and crack-free silica glass cylinder of roughly 5 mm-diameter and about 70 mm-length was obtained.

In order to use this sol-gel silica rod as a fiber core, an air/silica PCF was obtained using the conventional stack-and-draw process. At first, the sol-gel rod was stacked with pure silica capillaries in a hexagonal arrangement. The stack was then placed inside a silica jacket tube and drawn down to a cane, itself placed inside a silica jacket tube and drawn into a final fiber form. During the fiber manufacturing, the sol-gel rod was heated several times at high temperatures (around 2000°C). This fiber (SEM image presented in the inset of Fig. 3) has an outer diameter of 127 μm and a core diameter of 6.4 μm defined as the distance between two diametrically opposite holes. The pitch of the periodic cladding, Λ, and the diameter of the air holes, d, are 3.7 μm and 1.5 μm, respectively.

To control and validate the different phases involved in the entire process, we studied the optical responses of both preform and fiber samples.

Optical characterization of undoped and Cu-doped sol-gel silica rods: The obtained transparent glass rods were cut and polished into discs, as shown in the inset of Fig. 1.

Absorption spectra were recorded at room temperature using a Perkin-Elmer Lambda 19 UV-vis-IR double beam spectrometer.

Several set-ups based on UV excitation lines were used for photoluminescence (PL) and time-resolved analysis. Photoluminescence lifetime measurements were performed under excitation in the UV range (215 - 350 nm) by using a pulsed laser system (Spectra-Physics) with a pulse width of ~8 ns, a repetition rate of 10 Hz and an energy density per pulse of ~0.3 mJ cm^{-2}. The light emitted from the sample was dispersed by a spectrograph equipped with a 300 grooves/mm grating, blazed at 500 nm, and then acquired by an intensified charge coupled device (Princeton CCD) camera. The acquisition is gated within a time window of 3 μs width, which opens starting from an adapted delay time with respect to the laser pulse.

Optical characterization of the Cu-doped fiber: The spectral attenuation of the Cu-doped PCF was measured by the conventional cut-back technique using a white light source and an OSA. This measurement has been performed on a 2.5 m -long sample.

#176707 - $15.00 USD Received 21 Sep 2012; revised 21 Nov 2012; accepted 21 Nov 2012; published 20 Dec 2012

The copper ions location and distribution, over the PCF transverse cross section, were investigated through micro-photoluminescence measurements by using an Aramis (Jobin-Yvon) spectrometer equipped with a CCD camera, a He-Cd ion laser (energy 3.8 eV and power ~0.15 mW), a 2D micro-translation stage and a 40 × objective. All the spectra were acquired under experimental conditions ensuring a spatial resolution of the order of 10 µm.

To highlight the UV power effect on the visible emission intensity of copper ions, we transversally irradiated the fiber using a cw-UV laser operating at 244 nm with a beam diameter of about 0.8 mm. In this case, a 15 cm-length uncoated PCF sample was connected to the entrance slit of a sensitive and miniaturized spectrometer (QE 65000 from Ocean optics). This last and compact configuration is well adapted for rapid spectral analysis with an objective of dosimeter application.

3. Results and discussion

3.1. Bulk sol-gel glasses

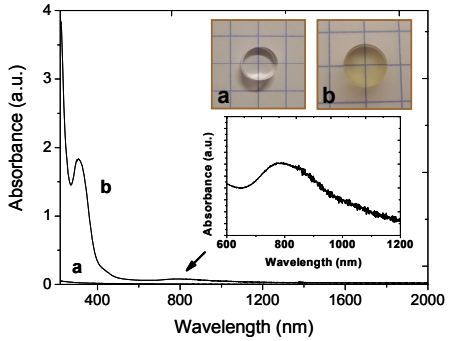

Fig. 1. Absorption spectra of (a) non-doped and (b) Cu-doped pure silica glasses. Insets present their corresponding photographs.

Figure 1 shows the absorption spectrum of the Cu-doped silica glass. The high optical quality of the elaborated samples is revealed over a broad spectral domain [200-2000] nm. The blank (non-doped) sample is almost transparent in the whole studied range whereas the Cu-doped one shows an intense UV absorption, revealing its potential use in UV-based detection systems. In comparison with the blank silica glass, the doped sample exhibits a narrow absorption band centered around 308 nm (2811 dB m^{-1}) and a broad one centered at about 800 nm (113 dB m^{-1}). These bands can be assigned to the ionic copper in a silicate glass. The first absorption band is attributed to monovalent Cu^{+} ion [15] and the second one to the divalent Cu^{2+} ion [16]. By using the absorption cross-sections reported in the literature [5] for both valences of copper ions in silicate glasses, absorption data made it possible to estimate the Cu^{2+} and Cu^{+} molar concentrations at 208 ppm and 12 ppm, respectively (molar ratio Cu^{n+}/Si). The mean copper molar concentration was estimated using electron probe microanalysis (EPMA) to be around 250 ppm. This value is close to that determined using optical characterizations.

#176707 - $15.00 USD Received 21 Sep 2012; revised 21 Nov 2012; accepted 21 Nov 2012; published 20 Dec 2012

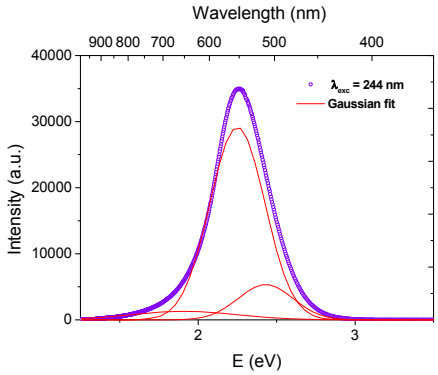

Fig. 2. Room temperature PL spectrum of a Cu-doped silica glass under 244 nm excitation wavelength.

The PL spectrum of a Cu-doped sol-gel silica glass, under laser excitation at 244 nm, is presented in Fig. 2. The strong band peaking at 550 nm with a Full Width at Half Maximum (FWHM) of about 100 nm is related to the transition from $3d^9 4s$ levels to the ground state of Cu^+ ions [17].

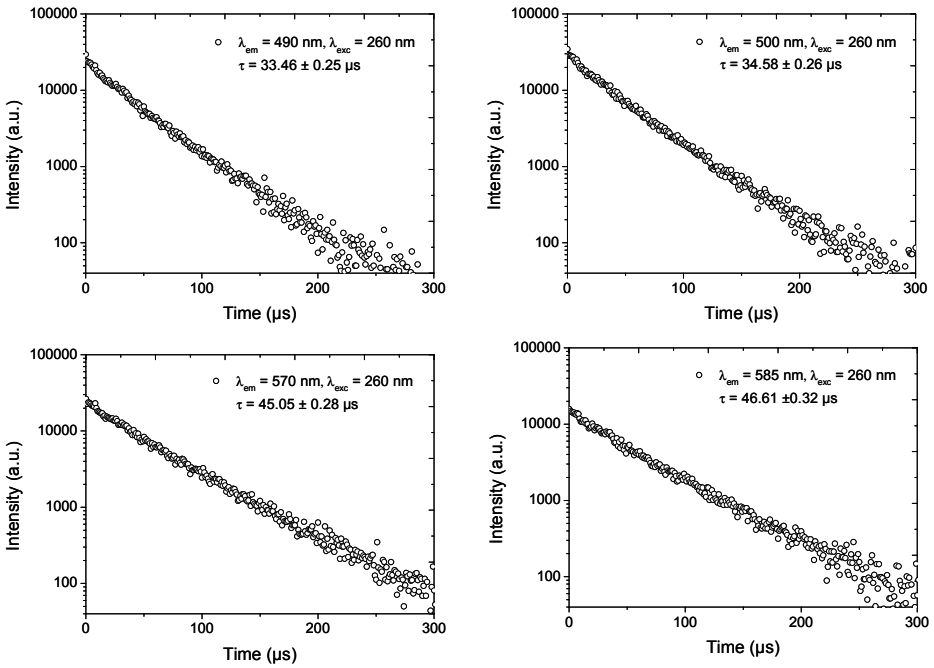

Fig. 3. PL kinetics of the Cu-doped bulk rod at different emission wavelengths (490, 500, 570 and 585 nm) under an excitation wavelength at 260 nm.

For a better analysis of the emitting centers within their surrounding medium, PL lifetime measurements were performed under excitation in the UV range. Some PL decay curves are reported in Fig. 3, for the sample excited by a pulsed laser at 260 nm and taken at 4 different emission spectral positions (490, 500, 570 and 585 nm). Those particular wavelengths have been chosen to scan the broad visible PL band. Even if all these kinetic evolutions can be correctly fitted with one exponential decay function, the calculated decay time undergoes a progressive evolution between 30 and 50 µs when the wavelength is increased. This behavior

#176707 - $15.00 USD Received 21 Sep 2012; revised 21 Nov 2012; accepted 21 Nov 2012; published 20 Dec 2012

seems to show that the emission band of Cu^{+} in Fig. 2 is in fact composed of two sub-bands. Actually, the dissymmetrical shape of this emission band is well fitted by three Gaussian bands centered at 511, 552 and 650 nm (Fig. 2) attributed to Cu^{+} ion and NonBridging Oxygen Hole Center (NBOHC) silica defects respectively. Such silica defect could be related to the presence of ionic coppers which break the Si-O-Si bonds in the host silica glass. This point appears more clearly and will be addressed in the following study of the doped optical fiber.

3.2. Copper-doped optical fiber

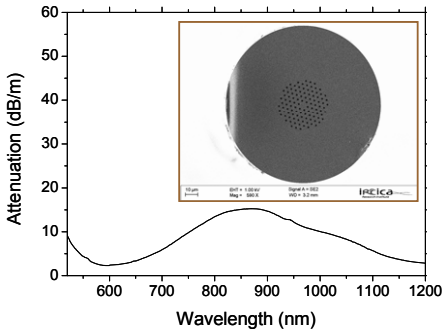

Fig. 4. Attenuation spectra of Cu-doped silica sol-gel core PCF. Inset: cross-section Scanning Electron Microscope (SEM) image of this fiber.

The optical attenuation spectrum of a Cu-doped PCF, drawn from the doped sol-gel silica rod, is shown in Fig. 4. This fiber presents a broad attenuation band between 600 and 1200 nm, which is assigned to Cu^{2+} ion, as already reported in the case of a MCVD conventional fiber [18]. The attenuation of this Cu^{2+}-related band was found to be around 13 dB m^{-1}. The optical spectrum analyzer (OSA) used to perform this measurement did not enable us to determine the Cu^{+} attenuation band in the PCF. By using the Cu^{2+} absorption cross-section coefficient [5], the measured attenuation and taking into account the overlap integral factor between the dopant and the optical mode (the factor calculated from the fiber data is 0.82), the molar concentration of Cu^{2+} ions in the PCF solid core is about 28 ppm (Cu^{2+}/Si). This concentration is one order of magnitude lower than in the corresponding sol-gel preform. This decrease in the Cu^{2+} concentration could be related to a reduction into the Cu^{+} state during the fiber drawing. Indeed, it has been proven that at high temperature, Cu^{+} and Cu^{2+} form an equilibrium with dissolved oxygen inside a melted glass ($4Cu^{2+} + 2O^{2-} \leftrightarrow 4Cu^{+} + O_2$) [19]. Hence, the $[Cu^{+}]/[Cu^{2+}]$ concentration ratio depends on different factors such as temperature, annealing time, compositions, etc [5]. During the fiber drawing, the sol-gel rod was heated several times at high temperatures (around 2000°C) under inert atmosphere. In this case, the absence of oxygen most likely shifts the thermodynamic equilibrium in favor of Cu^{+} formation. Therefore, by using the stack-and-draw process, the divalent state copper is converted into monovalent luminescent copper, suitable for UV radiation dosimetry.

#176707 - $15.00 USD Received 21 Sep 2012; revised 21 Nov 2012; accepted 21 Nov 2012; published 20 Dec 2012

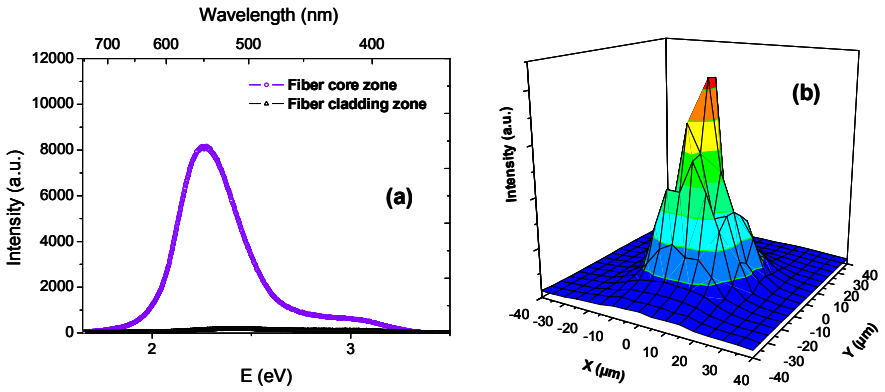

Fig. 5. (a) Room temperature μ-PL spectra of the Cu-doped PCF core and cladding zones (b) Spatial distribution of the μ-PL intensity recorded on the cross section of the Cu-doped PCF and integrated between 500 and 600 nm (λ_{exc} = 325 nm).

Besides, the presence of monovalent Cu^+ ions inside the core of the PCF was checked through micro-PL measurements in the visible region (Fig. 5(a)). One can note that the μ-PL spectrum of the Cu-doped fiber core zone, as compared to the one recorded in the cladding zone, presents the Cu^+-related PL band centered around 548 nm. The mapping of the Cu^+ distribution was investigated using the integrated intensity (Fig. 5(b)) of this luminescence and its maximum location is centered on the PCF core zone. Even if spatial resolution was not sufficient to accurately describe the fiber geometry, this clearly demonstrates that, after the fiber drawing, the ionic copper remains predominantly localized inside the sol-gel silica material.

For the luminescence-based UV-dosimetry measurements, the PCF was transversally irradiated by the UV incoming light. The spot position on the PCF was easily optimized via the diffraction picture just behind the irradiated fiber.

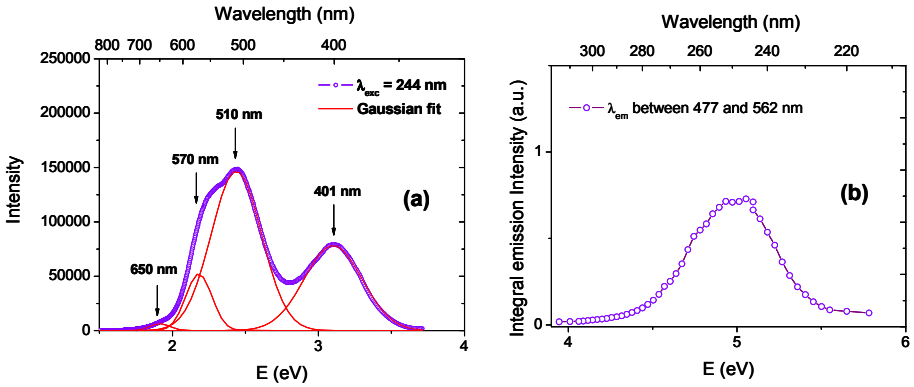

Fig. 6. (a) PL spectrum of Cu-doped PCF under excitation at 244 nm with an incident power of 100 mW (b) Excitation spectrum of the same PCF with the integral emission intensity between 477 and 562 nm.

In Fig. 6(b) is reported the excitation spectrum of Cu-doped PCF, which consists of a broad band centered at about 250 nm, attributed to Cu^+ ion [16]. Figure 6(a) presents the normalized visible PL spectrum of the same PCF under excitation at 244 nm, where two main and well-separated bands could be distinguished. The first one at 401 nm, with a FWHM of about 56 nm and a lifetime of 97 μs, was attributed to Oxygen Deficient Center silica defects (ODC) [20]. The second one, detected in the green domain, has a complex structure and is

#176707 - $15.00 USD Received 21 Sep 2012; revised 21 Nov 2012; accepted 21 Nov 2012; published 20 Dec 2012

related to the presence of Cu^{+} ions. This band can be decomposed in two Gaussian bands centered at 510 and 570 nm with a FWHM of about 89 and 67 nm, respectively. One can note also the presence of a weak band centered around 650 nm with a 10 µs lifetime. This last band is attributed to NonBridging Oxygen Hole Center (NBOHC) silica defects [21,22]. Such silica NBOHC could be generated by the fiber drawing process [23–26]. Hence, under 244 nm excitation, the Cu-doped PCF and the corresponding bulk preform present very different optical properties. In particular, as compared to the Cu-doped preform, the PCF exhibits an ODC band and strong changes in the shape of the Cu^{+}-associated band in the green region. These differences are induced by the fiber drawing process. In effect, while the densification under air (presence of oxygen) of the Cu-doped silica preform led to an insignificant amount of ODC centers, the fiber drawing was performed under inert atmosphere, which favors the formation of ODC silica defects. Such a generation of ODC defects by the fiber drawing process has been already demonstrated [27]. On the other hand, the FWHM of NBOHC-band is larger in the preform (Fig. 2) than in the corresponding PCF (Fig. 6(a)). This could be related to a site-to-site inhomogeneity, which leads to the broadening of the obtained bands. We can consider that the NBOHC defects, at the origin of the 650 nm PL band, are partially related to the dopants (Cu^{2+} and Cu^{+}), generating two class of defects with different surrounding environments. Since most of the divalent state copper is converted into monovalent luminescent copper during the drawing process, NBOHC tend to have one unique environment. Accordingly, this led to less site-to-site inhomogeneity and to a narrower band in the doped PCF compared to the preform.

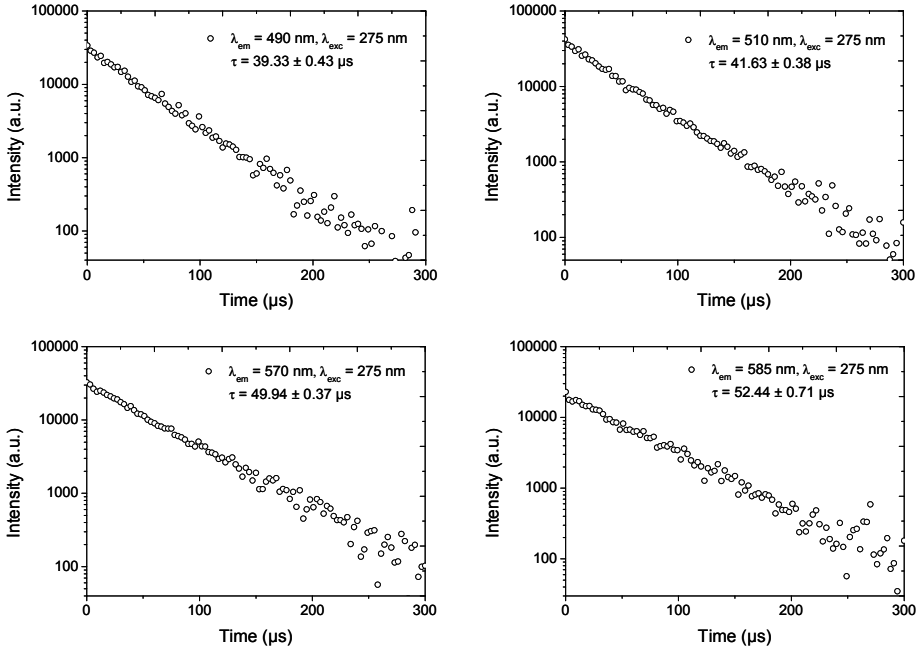

Fig. 7. PL kinetics of the Cu-doped PCF at different emission wavelengths (490, 510, 570 and 585 nm) under excitation at 275 nm.

In Fig. 7 are presented the results of PL decay measurements in the Cu-doped PCF excited at 275 nm for different emission wavelengths. In contrast to results obtained with Cu^{+} in sol-gel silica coatings [28] or in fused quartz glass [4], all decay curves fit a monoexponential function, suggesting a single emitting center in only one environment. The decay time progressively increases with the emission wavelength (Fig. 7). This evolution is related to the strong overlap between bands at 510 and 570 nm. Hence, it is likely that the real lifetimes from the levels corresponding to these bands are around 40 and 50 µs, respectively. However,

#176707 - $15.00 USD Received 21 Sep 2012; revised 21 Nov 2012; accepted 21 Nov 2012; published 20 Dec 2012

in the excitation conditions of experiments, the two levels influence each other, yielding an average lifetime between these extreme values. Note that such a mean value of the lifetime, as well as the absence of any dual-exponential behavior, is similar to the results reported in the case of a Cu^{+}-doped conventional fiber fabricated using granular oxide technique [29].

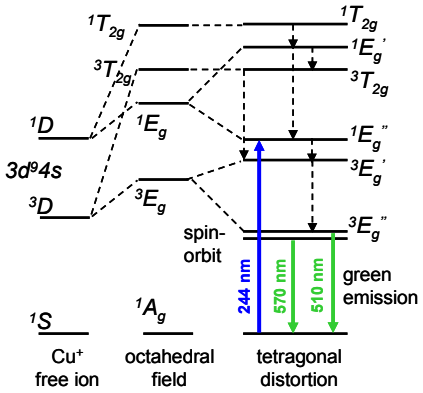

Fig. 8. Level configuration scheme for the Cu^{+} ion, with the effect of a tetragonal distortion of the octahedral field (Modified from ref [17].).

The Cu^{+} PL band structure may find its origin either in different surrounding configurations created by the fiber drawing or in the emission from different levels of the same center. It is known that the excited $3d^94s$ state of Cu^{+} ions are sensitive to the nature of the surrounding environment. The ligands field interactions split the excited state of Cu^{+} into $^1T_{2g}$, $^3T_{2g}$, ^1E_g, and ^3E_g levels. Moreover, the triplets can be further split by spin-orbit interaction, as illustrated in Fig. 8 [17]. As compared with crystals, silica glass has a random structure and bears inherent site-to-site inhomogeneity, which leads to the broadening of the obtained bands. However, the structure of the obtained PL band could be explained by tetragonal distortion of the Cu^{+} environment inside the silica glass PCF. The de-excitation from tetragonal distortion $^3E_g''$ levels is at the origin of the green emissions centered around 510 and 570 nm as illustrated in Fig. 8.

The obtained Cu-doped fiber has been tested for UV radiation dosimetry. To that purpose, the PL spectra were recorded under different laser powers.

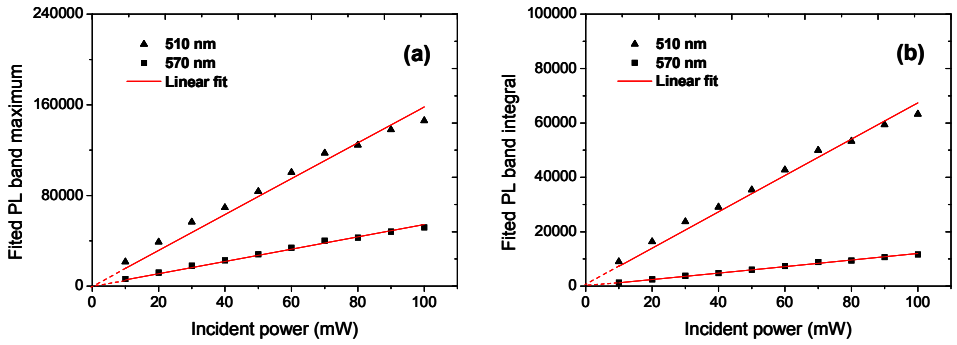

Fig. 9. Maximum (a) and integral (b) intensities of UV-induced luminescence fitted bands at 510 and 570 nm as a function of the excitation power (λ_{exc} = 244 nm).

The emission bands centered on 510 and 570 nm, respectively, have been monitored as a function of the 244 nm excitation incident powers. Fitted PL band intensity maxima and integrals are reported and both of them exhibit a linear response to a laser incident power up to 100 mW (Fig. 9) that corresponds to an irradiation power up to 2.7 mW on the Cu-doped

#176707 - $15.00 USD Received 21 Sep 2012; revised 21 Nov 2012; accepted 21 Nov 2012; published 20 Dec 2012

PCF core. Moreover, after several increase-and-decrease cycles of the laser power, these PL band intensity maxima and integrals were found to be totally reversible within the measurement accuracy of this study (± 1%). Such a highly sensitive and stable Cu-doped silica PCF could appear as a first device, paving the way for a remote and real-time measurement system of absorbed UV radiation doses.

4. Conclusion

In summary, a Cu^{+}/Cu^{2+}-doped silica PCF was achieved using an ionic copper-doped silica preform prepared by the polymeric sol-gel route. The fiber drawing conditions favor the conversion of Cu^{2+} into Cu^{+} ions inside the sol-gel silica glass, led to the apparition of ODC defect centers and gave a distortion of the silica tetragonal environment, resulting in a structuring of the green emission spectrum. The PL intensity of such an ionic Cu-doped PCF presented a good linear response to the UV incident power at 244 nm up to 100 mW at least, which makes it a potential candidate for radiation dosimetry applications in an all-fibered sensor configuration.

Acknowledgments

This work was supported by the French Agence Nationale de la Recherche (ANR) in the frame of the POMESCO project (Organized Photo-growth of Metallic and Semi-Conductor nano-objects intended to Optic devices), the “Conseil Régional Nord Pas de Calais Picardie” and the “Fonds Européen de Développement Economique des Régions”.

#176707 - $15.00 USD Received 21 Sep 2012; revised 21 Nov 2012; accepted 21 Nov 2012; published 20 Dec 2012